

Geophysical Research Letters[®]



RESEARCH LETTER

10.1029/2023GL104037

Key Points:

- A Linear Inverse Model is used to decompose and compare tropical Pacific decadal variability dynamics in observations and climate models
- Coupled Model Intercomparison Project Phase 6 models have significant challenges in reproducing the observed dynamics and spatial pattern of tropical Pacific decadal variability
- Many models (>50%) cannot reproduce the roles of extratropics-tropics coupling and thermocline variability in tropical Pacific variability

Supporting Information:

Supporting Information may be found in the online version of this article.

Correspondence to:

Y. Zhao,
zhaoyw1@163.com





Citation:

Zhao, Y., Di Lorenzo, E., Newman, M., Capotondi, A., & Stevenson, S. (2023). A Pacific tropical decadal variability challenge for climate models. *Geophysical Research Letters*, 50, e2023GL104037. <https://doi.org/10.1029/2023GL104037>

Received 7 APR 2023

Accepted 19 JUL 2023

A Pacific Tropical Decadal Variability Challenge for Climate Models

Yingying Zhao¹ , Emanuele Di Lorenzo², Matthew Newman³ , Antonietta Capotondi^{3,4} , and Samantha Stevenson⁵ 

¹Laoshan Laboratory, Qingdao, China, ²Department of Earth, Environmental, and Planetary Sciences, Brown University, Providence, RI, USA, ³Physical Sciences Laboratory, NOAA, Boulder, CO, USA, ⁴CIRES, Cooperative Institute for Research in Environmental Sciences, University of Colorado at Boulder, Boulder, CO, USA, ⁵Bren School of Environmental Science and Management, University of California, Santa Barbara, Santa Barbara, CA, USA

Abstract Understanding and forecasting Tropical Pacific Decadal-scale Variability (TPDV) strongly rely on climate model simulations. Using a Linear Inverse Modeling (LIM) diagnostic approach, we reveal Coupled Model Intercomparison Project Phase 6 models have significant challenges in reproducing the spatial structure and dominant mechanisms of TPDV. Specifically, while the models' ensemble mean pattern of TPDV resembles that of observations, the spread across models is very large and most models show significant differences from observations. In observations, removing the coupling between extratropics and tropics reduces TPDV by ~60%–70%, and removing the tropical thermocline variability makes the central tropical Pacific a key center of action for TPDV and El Niño Southern Oscillation variability. These characteristics are only confirmed in a subset of models. Differences between observations and simulations are outside the range of natural internal TPDV noise and pose important questions regarding our ability to model the impacts of natural internal low-frequency variability superimposed on long-term climate change.

Plain Language Summary Tropical Pacific Decadal-scale Variability (TPDV) has been shown to impact global-scale climate fluctuations, weather regimes, and temperature trends such as the 1998–2012 global warming hiatus. Understanding and predicting TPDV's impacts strongly rely on climate model simulations and projections. However, the models show key deficiencies in reproducing the observed structure of TPDV. Although the arithmetic mean of TPDV's spatial pattern in each individual model is similar to observations, there is a large spread among models, and most models show significant differences from observations. Using an empirical dynamical model to decompose the mechanisms of the climate models reveals that more than 50% of the models fail to reproduce the roles of extratropics-tropics coupling and the tropical thermocline variability play in TPDV. These differences show significant challenges exist across the models for modeling the decadal-scale climate variability in the tropical Pacific. Improving the simulation of TPDV in climate models is vital for understanding the impacts of natural internal low-frequency variability alongside long-term climate change.

1. Introduction

Tropical Pacific decadal-scale variability (TPDV) on timescales longer than 6–8 years plays an important role in modulating global climate and regional weather and marine ecosystems, with important societal impacts (Alexander et al., 2002; Capotondi et al., 2020; Di Lorenzo et al., 2013; Fisman et al., 2016; Liu & Di Lorenzo, 2018; Power et al., 1999, 2021; Vimont, 2005). TPDV also impacted the growth rate of globally averaged surface air temperature over the past century, significantly contributing to the observed global warming hiatus of the early 2000s (England et al., 2014; Kosaka & Xie, 2013; Meehl et al., 2013; Watanabe et al., 2014). Previous work has extensively studied the mechanisms of TPDV based on observational data and model simulations, finding that both internal tropical atmosphere-ocean coupled dynamical processes (Li et al., 2006; Liu et al., 2002; Wu et al., 2003) and extratropical-tropical interactions (e.g., Chung et al., 2019; Liguori & Di Lorenzo, 2019; Sun & Okumura, 2019; Zhao & Di Lorenzo, 2020) play an important role in driving TPDV. In particular, previous studies based on observational data found that extratropical El Niño Southern Oscillation (ENSO) precursor dynamics are estimated to explain about 65% of TPDV (Di Lorenzo et al., 2015; Zhao & Di Lorenzo, 2020). In the subtropical region, the thermodynamic ocean-atmosphere coupling (e.g., the wind-evaporation-sea surface temperature (SST) feedback (WES feedback), Xie and Philander 1994) is a key driver of the extratropical ENSO

© 2023. The Authors.

This is an open access article under the terms of the [Creative Commons Attribution-NonCommercial-NoDerivs License](https://creativecommons.org/licenses/by-nc-nd/4.0/), which permits use and distribution in any medium, provided the original work is properly cited, the use is non-commercial and no modifications or adaptations are made.

precursors by activating the seasonal foot-printing mechanism (SFM) (Vimont et al., 2001, 2003) and leading to Meridional Modes (MMs) (Chang et al., 2007; Chiang & Vimont, 2004). The MMs have been shown to play an important role in energizing ENSO and TPDV (e.g., Ding et al., 2015; Liguori & Di Lorenzo, 2019; Liu & Di Lorenzo, 2018). Besides, the thermocline variability also contributes to the tropical Pacific SST variance at both interannual and decadal timescales mainly through the dynamical coupling, involving the thermocline feedback (e.g., An & Jin, 2001; Jin & An, 1999) and the changes in the sub-tropical cells through the wind-induced off-equatorial Rossby waves (Anderson et al., 2013; Capotondi & Qiu, 2022).

The relatively short instrumental record for the tropical Pacific (Deser et al., 2010) makes long-term simulations from Earth System Models (ESMs) powerful tools to understand TPDV. However, recent studies show climate models from Phase 5 of the Coupled Model Intercomparison Project (CMIP5) display major deficiencies in simulating TPDV (Henley et al., 2017; Lyu et al., 2016; Power et al., 2021; Zhao, Di Lorenzo, et al., 2021), preventing a complete characterization and understanding of TPDV. For example, the simulated equatorial Pacific warming in most models extends too far to the west (Lyu et al., 2016; Power et al., 2021); the magnitude of TPDV varies markedly from model to model and is underestimated by most models (Power et al., 2021; Zhao, Di Lorenzo, et al., 2021); and most models underestimate the contribution of the extratropical precursor dynamics to the TPDV (Zhao, Di Lorenzo, et al., 2021). However, most studies only examined the simulated spatial-temporal characteristics of TPDV, and fewer diagnosed the mechanisms of TPDV among the climate models. Moreover, to our knowledge, there is no study diagnosing the simulation of TPDV among the Coupled Model Intercomparison Project Phase 6 (CMIP6) models. In this work, we evaluate the mechanisms of TPDV across CMIP6 climate model simulations and compare them with those inferred from observations.

Since the physical interactions between the extratropical Pacific and tropical Pacific occur on a wide range of spatial and temporal scales (e.g., Liu & Di Lorenzo, 2018; Newman et al., 2016), this paper uses a diagnostic approach based on a multivariate dynamical system—Linear Inverse Model (LIM) described in Zhao, Newman, et al. (2021) to explore the mechanisms of TPDV, that is, the roles of tropical dynamics versus extratropical dynamics, and the roles of thermocline variability versus surface fluxes including the thermodynamical coupling. In this work, we first evaluate the representation of TPDV in 31 CMIP6 climate models to understand how well they are able to capture observed TPDV. Then the LIM approach is used to explore the mechanisms of TPDV in climate models and compare them to those in the observations.

2. Data and Method

2.1. Observation and Model Data

Monthly mean values of SST (unit: °C) and SSH (unit: m) from the European Centre for Medium-Range Weather Forecasting (ECMWF) Ocean Reanalysis System 4 (ORAS4) (Balmaseda et al., 2013) for the period January 1958 to December 2014 are used in this study. The model data include monthly mean SST and SSH output from historical simulations (r1i1p1) of 31 climate models from Phase 6 of the Coupled Model Intercomparison Project (CMIP6) (Eyring et al., 2016) (Table S1 in Supporting Information S1). The period of model data is from January 1958 to December 2014. SST and SSH fields are first averaged into 2° latitude × 5° longitude grid boxes. The anomalies are derived by removing the climatological seasonal cycle. Before performing the empirical orthogonal function (EOF) analysis, each field is normalized by its domain-averaged climatological STD. The externally forced trend is removed following Penland and Matrosova (2016) and Frankignoul et al. (2017) (Text S1 in Supporting Information S1). Then the LIM is constructed by principal component (PC) time series derived from the EOF analysis.

2.2. Linear Inverse Model

The LIM framework can be applied to the climate system where the nonlinear dynamics decorrelate much faster than the linear dynamics, which can be approximated as a multivariate linear dynamical system driven by white noise (Hasselmann, 1976; Penland & Sardeshmukh, 1995):

$$\frac{dx}{dt} = Lx + \xi, \quad (1)$$

where x is the state vector, L is the linear dynamical operator defining the evolution of x , and ξ is the white noise forcing. Following Penland and Sardeshmukh (1995), the matrix L is determined by:

$$L = \tau_0^{-1} \ln \{ C(\tau_0) C(0)^{-1} \}, \quad (2)$$

where $C(0)$ and $C(\tau_0)$ represent the covariance matrices and lag-covariance matrix at lag τ_0 , respectively—that is, $C(0) = \langle x(t)x^T(t) \rangle$ and $C(\tau_0) = \langle x(t + \tau_0)x^T(t) \rangle$, where $\tau_0 = 1$ month.

To simulate the dynamics of the coupled system of tropical Pacific and extratropical Pacific, we rewrite Equation 1 as:

$$\frac{dx}{dt} = \frac{d}{dt} \begin{bmatrix} x_T \\ x_N \\ x_S \end{bmatrix} = \begin{bmatrix} L_{TT} & L_{NT} & L_{ST} \\ L_{TN} & L_{NN} & L_{SN} \\ L_{TS} & L_{NS} & L_{SS} \end{bmatrix} \begin{bmatrix} x_T \\ x_N \\ x_S \end{bmatrix} + \begin{bmatrix} \xi_T \\ \xi_N \\ \xi_S \end{bmatrix}, \quad (3)$$

where x_T , x_N and x_S represent the variables within the tropical Pacific (20°S–14°N), North Pacific (16°N–60°N), and South Pacific (60°S–22°S), respectively. Note here we used an asymmetrical tropical region from 20°S to 14°N because 20°S and 14°N (gray lines in Figure S1a in Supporting Information S1) can separate the tropical SST variance and extratropical SST variance more clearly in observations, and have been used in previous studies (e.g., Lou et al., 2020; Lou et al., 2021; Zhao, Newman, et al., 2021). Furthermore, the results of the region experiment show that the main results are not qualitatively changed when using different dividing lines (Figure S2, Text 2 in Supporting Information S1). Following Zhao, Newman, et al. (2021), we constructed the state vector x using 12/3/12/2/12/2 leading PCs of $SST_T/SSH_T/SST_N/SSH_N/SST_S/SSH_S$ (hereafter Full LIM), which explains 87/65/69/24/73/36 percent of the variability of their respective fields. Note that using slightly different EOF truncations does not qualitatively change the tropical Pacific SST variances in the LIMs (Figure S3 and Text 2 in Supporting Information S1).

We next separate the contributions of different physical processes to tropical Pacific climate variability using the LIM. To explore the role of extratropics-tropics coupling, we construct a TP-only LIM, where all interactions between tropical and extratropical Pacific are removed. Similarly, to investigate impacts of the tropical Pacific thermocline variability, we build the No-SSH LIM1 (No-SSH LIM2) where the impact of tropical and extratropical SSH (only extratropical SSH) on the tropical Pacific climate variability is removed. The details are described in Text S3 in Supporting Information S1. Note that before using the LIMs for diagnosis, we conduct a “tau test” (Penland & Sardeshmukh, 1995) to examine the validity of the linear approximation (Figure S1 and Text S4 in Supporting Information S1). Then the 100-member sets of LIM reconstructions are constructed, which are then used for analyzing the decoupled low-frequency variance and for significance testing in a standard Monte Carlo approach (Text 5 in Supporting Information S1).

We next build LIMs from the output of each CMIP6 model and repeated the observational LIM analysis. The LIM can represent the tropical Pacific low-frequency SST variance in CMIP6 models and therefore can be used to diagnose the simulation of the TPDV (Figures S4 and S5, Text S6 in Supporting Information S1). To better investigate the TPDV in CMIP6 models, we classify the models into two groups according to the differences between the total low-frequency SST variance and the TP-only low-frequency SST variance within 10°S–10°N. Models where the spatial mean of the differences is positive and larger than 0.01 (°C²) are classified into Group One, while models where the spatial mean is negative are classified into Group Two (Table S1 in Supporting Information S1). Hence, in Group One models, extratropical dynamics have an important overall positive contribution to the TPDV, while in Group Two models, the overall contribution is negative.

3. The Role of Tropical Atlantic in CP and EP ENSO Prediction and PB

3.1. The Representation of TPDV Across CMIP6 Models

In this section, we first examine the models' sea surface temperature (SST) variance pattern and compare them to observations (Figure S6 in Supporting Information S1) to diagnose the representation of tropical Pacific climate variability among CMIP6 models. Although the SST variance is stronger or weaker in some models compared to observations, most CMIP6 models can represent the basic ENSO-like pattern of the SST variance (Figure S6 in Supporting Information S1) and the multi-model ensemble mean (MEM) pattern closely resembles the observations. We then examine the tropical Pacific low-frequency SST variance in CMIP6 models (Figure 1) to identify the features of TPDV. We apply the Zhang et al. (1997) low-pass filter to SST anomaly (SSTa) from observations and CMIP6 output to filter out higher frequencies (periods <6 years) including those associated

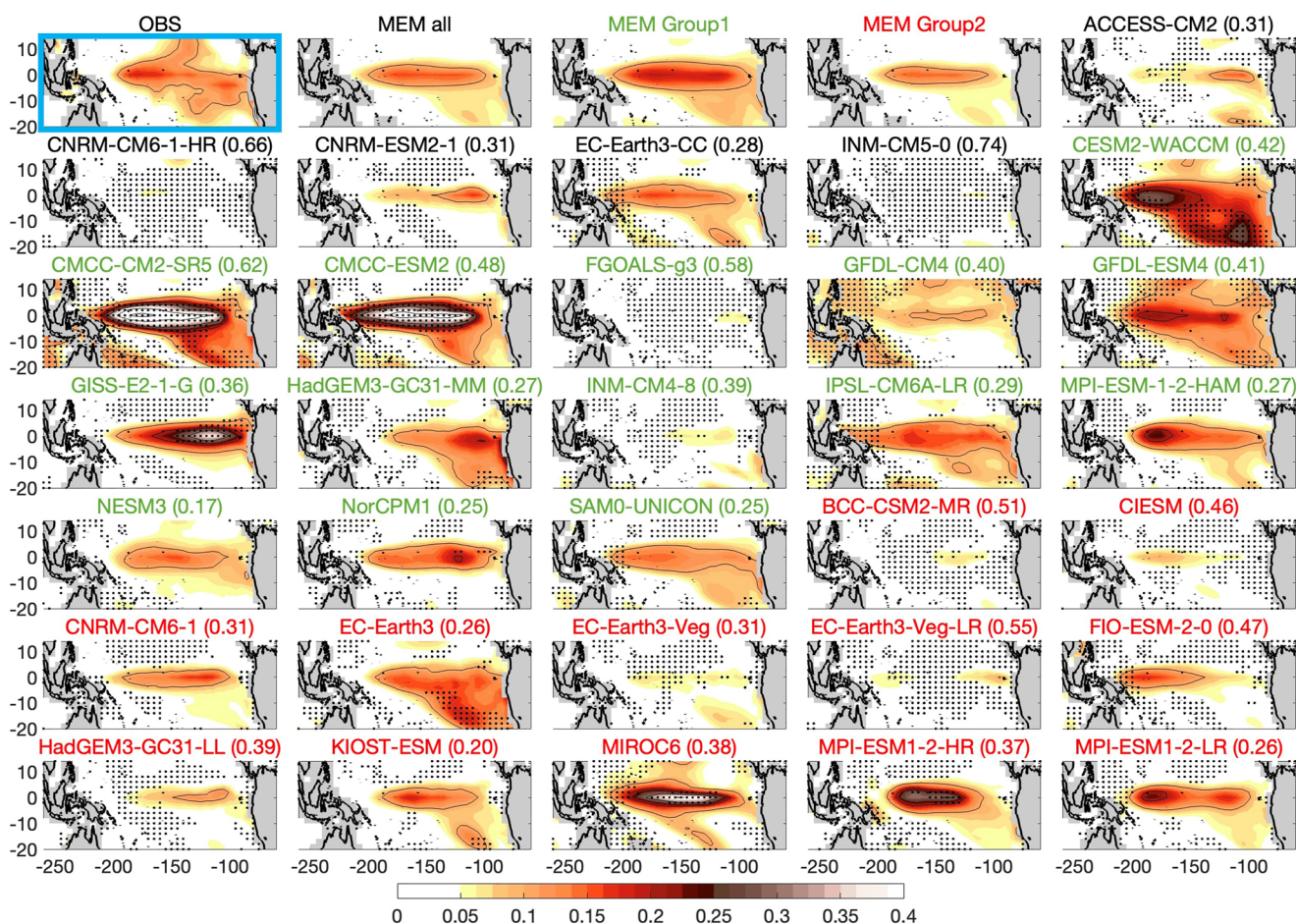


Figure 1. Tropical Pacific low-frequency SST variance ($^{\circ}\text{C}^2$) of observation (OBS) from ORAS4; models ensemble mean of all models (MEM all), Group One models (MEM Group One), and Group Two models (MEM Group Two); and each CMIP6 model. The pattern of OBS is highlighted with a blue outline. Models with the green (red) title are Group One (Group Two) models. The gray dots in patterns of CMIP6 models show that the simulated low-frequency SST variance is different from the observations at 95% significance level. The number in each subtitle shows the fraction of the area that is significantly different from the observation.

with ENSO inter-annual variability. Note that similar results were obtained when using the 8-year lowpass filter (figures not shown).

Although most models can capture the characteristics of the tropical Pacific SST variance, there are significant differences in the representation of the TPDV across CMIP6 models when compared to observations (Figure 1). The TPDV in some models is much stronger than observed (e.g., CESM2-WACCM, CMCC-CM2-SR5, CMCC-ESM2), while in some models is much weaker (e.g., CNRM-CM6-1-HR, INM-CM5-0, FGOALS-g3). Most models have a reduced loading of variance in the Central North Pacific consistent with the excitation region of the North Pacific extra-tropical precursor dynamics (e.g., Di Lorenzo et al., 2015; Liu & Xie, 1994), suggesting that these models underestimate the role of North Pacific precursors in TPDV. On the contrary, many models can capture the low-frequency variance in the Southeast Pacific, where several dynamics can energize the SST variance, for example, the South Pacific precursor dynamics (Zhang et al., 2014), and the reddening of the South Pacific extra-tropical trade winds (Okumura, 2013). Overall, the TPDV pattern in most CMIP6 models shows significant differences from observations (see gray dots in Figure 1 and Methods section for the definition of significance), suggesting that these models display major deficiencies in simulating key aspects of TPDV. Nevertheless, the MEM low-frequency SST variance, which is averaged across models is similar to the observations (Figure 1) despite the significant differences across the model variance pattern.

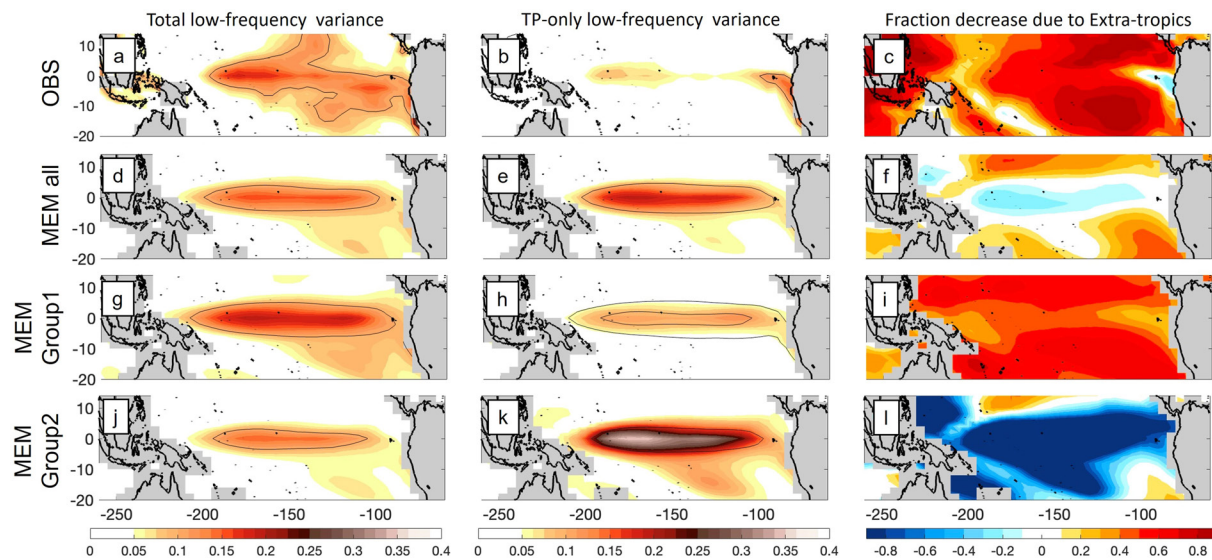


Figure 2. Low-frequency SST variance ($^{\circ}\text{C}^2$) in the tropical Pacific basin of (a) observation, (d) MEM of all CMIP6 models, (g) MEM of Group One models, and (j) MEM of Group Two models. The decoupled low-frequency SST variance ($^{\circ}\text{C}^2$) in the tropical Pacific basin of (b) observation, (e) MEM of all CMIP6 models, (h) MEM of Group One models, and (k) MEM of Group Two models. Fraction decrease from the total low-frequency SST variance to decoupled low-frequency variance of (c) observation, (f) MEM of all CMIP6 models, (i) MEM of Group One models, and (l) MEM of Group Two models.

3.2. Extra-Tropical Forcing of Tropical Pacific Decadal-Scale Variability

The previous section shows that the representation of TPDV in CMIP6 models greatly differs from observations and across models (Figure 1). This raises the possibility that the mechanisms of TPDV in CMIP6 models may also be different from the observations and from model to model.

Previous observational studies suggest that the largest fraction of TPDV ($\sim 65\%$) is sourced from extratropical ENSO precursors (Di Lorenzo et al., 2015; Zhao & Di Lorenzo, 2020). To evaluate the overall impact of extratropical dynamics on tropical Pacific decadal-scale variability, we use the LIM diagnostic model (see Methods) to separate the contributions to TPDV arising from tropically confined dynamics only (TP-only LIM) versus those arising from coupled tropical/extratropical interactions (Figure 2). In observations, the low-frequency SSTa variance has comparatively higher amplitude in the central tropical Pacific (near the dateline) than in the eastern tropical Pacific (Figure 2a). In comparison, the TP-only low-frequency variance is sharply reduced in most regions of the tropical Pacific (Figure 2b). When comparing the total TPDV (Figure 2a) to the one linked to local tropical dynamics only (Figure 2b), we find that in the observations the tropical-extratropical feedbacks explain the largest fraction of TPDV SSTa variability ($\sim 60\text{--}70\%$, Figure 2c, shows the fraction difference between the full state and TP-only LIM), which is consistent with previous statistical estimates based on observations alone (Zhao & Di Lorenzo, 2020).

The CMIP6 models substantially underestimate the contribution of extratropical dynamics to the TPDV, relative to observations. For the MEM of all the CMIP6 models, the TP-only variance is increased compared to the total SST variance (cf. Figures 2d and 2e) with an increase of about 20% in the equatorial region (Figure 2f), in contrast with the decrease seen in observations (Figure 2c). After inspecting each individual model in CMIP6 (Figures S7 and S8 in Supporting Information S1), we find that the patterns of the local low-frequency SST variance from the TP-only LIM vary markedly from model to model (Figure S7 in Supporting Information S1). When removing the impact of extratropical dynamics, the local low-frequency SST variance is significantly increased in some models compared to the total low-frequency variance, while in other models is decreased (Figure S8 in Supporting Information S1). More than 50% of the models cannot reproduce the contribution of extratropical dynamics to the TPDV in observations (Figure S8 in Supporting Information S1). This suggests that the mechanisms of TPDV are very different among the CMIP6 models.

The MEM of Group One models exhibits stronger low-frequency SST variance compared to the MEM of Group Two models (Figure 2g vs. Figure 2j), and the decoupling of tropics—extratropics leads to a significant reduction

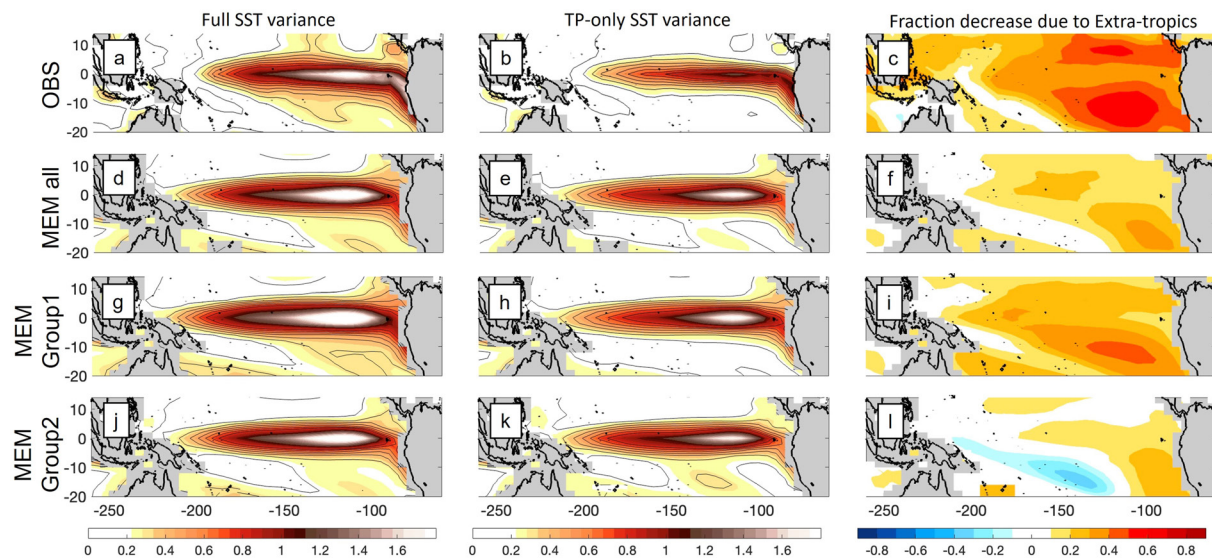


Figure 3. Full SST variance ($^{\circ}\text{C}^2$) in the tropical Pacific basin of (a) observation, (d) MEM of all CMIP6 models, (g) MEM of Group One models, and (j) MEM of Group Two models. Here the full SST variance means the variance including all frequencies. The decoupled SST variance ($^{\circ}\text{C}^2$) in the tropical Pacific basin of (b) observation, (e) MEM of all CMIP6 models, (h) MEM of Group One models, and (k) MEM of Group Two models. Fraction decrease from full SST variance to the decoupled variance of (c) observation, (f) MEM of all CMIP6 models, (i) MEM of Group One models, and (l) MEM of Group Two models.

in the TPDV ($\sim 50\%$ – 60% , Figure 2i), which is consistent with observations (Figure 2c). Different behavior is seen in the Group Two models, where the lack of tropical-extratropical coupling leads to a strong increase in the TPDV (Figures 2k and 2l). These results suggest that while extratropical dynamics play an important role in shaping the TPDV in Group One models, in Group Two the extratropical dynamics seem to be acting as a source of noise to the TPDV or a coherent dynamical process which tends to damp TPDV—that is the absence of the extratropical noise leads to stronger TPDV. The other CMIP6 models are far less sensitive to extratropical forcing implying that their TPDV is primarily reflective of internal tropical processes.

3.3. Extra-Tropical Forcing of Full Tropical Pacific Variability

Next, we examine the impact of extra-tropical dynamics on the tropical Pacific full SST variance (Figure 3), that is including both ENSO and TPDV timescales. In observations, the full SST variance has a high amplitude in the cold tongue region and extends to the warm pool region with decreasing amplitude (Figure 3a). After removing the extratropical influence, the TP-only SST variance (Figure 3b) is substantially reduced, and more concentrated in the equatorial Pacific region compared to the total variance (Figure 3b vs. 3a). A substantial fraction of tropical SST variance relies on coupling with the extra-tropics, especially in the eastern tropical Pacific region ($\sim 40\%$) (Figure 3c). We then remove the low-frequency SST variance from the full variance and find that the extratropical dynamics can explain about 30%–40% of the SST variance on the ENSO timescale (Figure S9 in Supporting Information S1).

In the full suite of CMIP6 models, similar to what was found for TPDV, the total SST variance is less impacted by the extratropical coupling than in observations. The representation of local SST variance in each CMIP6 model is different from the observations and each other (Figure S10 in Supporting Information S1). The fraction decreases from the full SST variance (Figure S6 in Supporting Information S1) to TP-only variance (Figure S10 in Supporting Information S1) due to the extratropical influence is much smaller when compared to the fraction decrease of low-frequency variance (Figure S11 vs. Figure S8 in Supporting Information S1), and is positive in most models (Figure S11 in Supporting Information S1), indicating that extratropical dynamics contribute to the tropical Pacific climate variability in these models (e.g., on ENSO timescales). However, in the MEM of all CMIP6 models, the change in local SST variance is relatively small compared to the full SST variance (cf. Figures 3d and 3e), with a reduction of only about 10%–20% in the eastern tropical Pacific (Figure 3f). This suggests that, in general, tropical Pacific SST variability is considerably less influenced by extratropical dynamics in CMIP6 models compared to observations (cf. Figures 3c and 3f). If we examine the Group One and Group

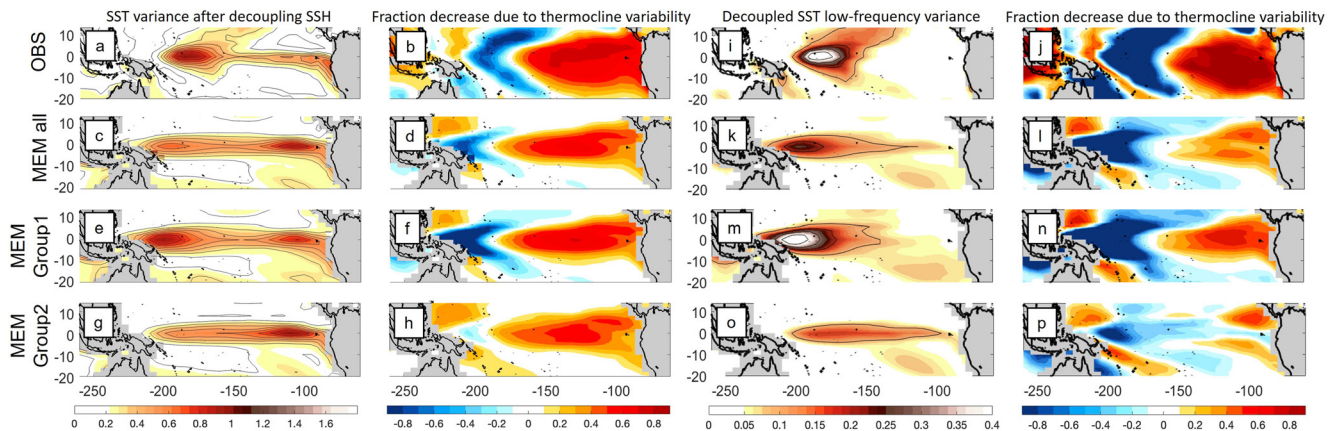


Figure 4. The tropical Pacific SST variance ($^{\circ}\text{C}^2$) when removing the impact of SSH of (a) observation, (c) MEM of all CMIP6 models, (e) MEM of Group One models, and (g) MEM of Group Two models. Fraction decrease from full SST variance to SST variance when removing the impact of SSH of (b) observation, (d) MEM of all CMIP6 models, (f) MEM of Group One models, and (h) MEM of Group Two models (i–p) Similar to (a–h) but for the tropical Pacific low-frequency SST variance ($^{\circ}\text{C}^2$) when removing the impact of SSH.

Two MEM separately, we find that in Group One the extratropical dynamics play a more important role in driving full tropical Pacific variability compared to that in Group Two (cf. Figures 3i and 3l). Overall, we find that in Group One models, the extratropical dynamics significantly impact tropical variability at both interannual and decadal timescales.

3.4. Thermocline Variability Versus Surface Dynamics in Tropical Pacific Climate Variability

To further diagnose the differences of tropical Pacific climate variability in CMIP6 models and observations, No-SSH LIM1 is conducted where both the tropical and extra-tropical SSH is decoupled from the SST. By decoupling the SSH and SST, we are allowed to separate the effect of thermocline variability including the trade wind charging mechanism (Anderson et al., 2013) from the surface dynamics including the thermodynamic coupling between tropics and extratropics (e.g., the WES feedback), which has been shown to be a key driver of the extra-tropical ENSO precursors (Chang et al., 2007; Chiang & Vimont, 2004; Vimont et al., 2001, 2003).

In the observations, when there is no thermocline variability, the surface dynamics alone leads to a pattern that exhibits a strong core of action in the central tropical Pacific consistent with the excitation region of the Meridional Modes (Figure 4a) (e.g., Di Lorenzo et al., 2015; Liu & Di Lorenzo, 2018; Liu & Xie, 1994). If we examine the spatial changes in variance in observations (Figure 4b), we find that the variance in the eastern tropical Pacific is reduced by a large portion ($>60\%$). This suggests that the lack of thermocline variability reduces the ENSO feedbacks that are important in shaping the eastern equatorial variance (e.g., the thermocline feedback) through the eastward propagation of equatorial Kelvin waves. To further diagnose the impact of tropical/extratropical SSH in observations, we build a No-SSH LIM2 in which only the extratropical SSH is decoupled from the tropical Pacific climate system (Figure S12 in Supporting Information S1). In this LIM, the decoupled SST variance closely resembles the full SST variance (cf. Figures S12a and S12b in Supporting Information S1) with a small reduction mainly in the off-equatorial region (Figure S12c in Supporting Information S1). This indicates that the extratropical thermocline variability plays a much less important role in shaping the tropical Pacific SST variance compared to the tropical thermocline variability. From this analysis, we infer that thermodynamical coupling processes between extratropics and tropics (e.g., the WES feedback) inject energy into the central equatorial Pacific, which is transferred to the eastern tropical Pacific mainly via the tropical dynamical processes (e.g., equatorial Kelvin waves).

In the CMIP6 MEM, we find that the surface dynamics alone energizes variance in two centers of action along the equator, one in the east and one in the west side of the basin (Figure 4c), with much weaker variance in the central Pacific, as seen in observations, and stronger variance in the eastern equatorial Pacific compared to observations (cf. Figures 4c and 4a). In CMIP6 models, the thermocline variability is important to the tropical Pacific SST variance, contributing a large fraction ($\sim 40\%$ – 60% east of the dateline) of the full variance in the

MEM (Figure 4d), but its impact is not as profound as that in the observations (Figure 4b vs. 4d). Specifically, the Group One models are able to capture the strong SST variance due to the thermodynamical coupling in the central tropical Pacific but with a center displaced westward (cf. Figures 4a and 4e), while Group Two models cannot capture the pattern but rather show an ENSO-like pattern extending into the east with a center of action off the coast of South America (cf. Figures 4a and 4g). Moreover, the thermocline variability contributes a larger fraction of the tropical Pacific SST variance in Group One models east of the dateline compared to Group Two models (cf. Figures 4f and 4h).

We now re-examine the SST variance patterns by applying a 6-year low-pass filter to the LIM output to inspect the impacts of thermocline variability/surface dynamics on TPDV (Figures 4i–4p). Consistent with previous studies suggesting that the extratropical ENSO precursors and Meridional Modes are a key source of TPDV in the central tropical Pacific (Di Lorenzo et al., 2015; Zhao & Di Lorenzo, 2020), we find that the low-frequency SST variance after decoupling the SSH is characterized by a very strong center in the central tropical Pacific near the dateline (Figure 4i), which is consistent with the excitation region of the Meridional Modes (e.g., Di Lorenzo et al., 2015; Liu & Di Lorenzo, 2018; Liu & Xie, 1994). However, the variance in the eastern tropical Pacific is much weaker and almost insignificant compared to the full TPDV variance (cf. Figures 4i and 2a). Without the thermocline variability, the energy “injected” in the central equatorial Pacific by thermodynamical processes in the LIM cannot propagate eastward through equatorial Kelvin waves and remains trapped in the central-western Pacific, as seen for the full variability in Figure 4a. Therefore, the thermocline variability exhibits a strong positive (negative) contribution to the low-frequency SST variance in the eastern (central) tropical Pacific region (Figure 4j).

When comparing the observational finding to the CMIP6 MEM, we find that the low-frequency SST variance driven by the surface dynamics shows important differences, and the contribution of thermocline variability to the TPDV is greatly underestimated by CMIP6 models (Figures 4k and 4l). After removing the thermocline variability, the MEM of all CMIP6 models shows weaker (stronger) low-frequency SST variability in the central (eastern) tropical Pacific region compared to observations (cf. Figures 4k and 4i). Therefore, the fraction increase (decrease) due to the thermocline variability in the central (eastern) tropical Pacific region is much smaller in MEM (cf. Figures 4i and 4j). This suggests that the thermocline variability may play a much less important role in shaping the TPDV in most CMIP6 models compared to the observations. To be more specific, the observed low-frequency SST variance after decoupling SSH is well reproduced by Group One models, but the center of action is more westward (cf. Figures 4m and 4i), while that in Group Two models is greatly different from the observations, showing an ENSO-like pattern extending into the east (Figure 4o). In Group One models, the thermocline variability can explain a much larger fraction of TPDV when compared to Group Two models (cf. Figures 4n and 4p). These results suggest again that the Group One models, in which extratropical dynamics are important in driving TPDV, tend to better simulate the different roles that the surface dynamics and thermocline variability play in shaping TPDV.

4. Summary and Discussion

Using an empirical dynamical model (LIM) that allowed us to selectively include or exclude the extratropical coupling and the thermocline variability, we examine the representation of tropical Pacific climate variability, especially TPDV, in CMIP6 models. To summarize our results, we compare the patterns of tropical Pacific total and low-frequency SST variances in each CMIP6 model (diamonds) to the observed (black pentagrams) using Taylor diagrams (Figure S13 in Supporting Information S1).

The CMIP6 models (diamonds in Figure S13a in Supporting Information S1) can basically reproduce the observed SST variance pattern (black pentagram in Figure S13a in Supporting Information S1), with the spatial correlation coefficient (SCC, cosine of the angles from the x -axis) in most models larger than 0.8. Tropical-extratropical coupling drives a large fraction of the tropical Pacific climate variability in observations (Figures 3a–3c). However, after removing the tropical-extratropical coupling, the large scatter of points in the Taylor diagram (Figure S13b in Supporting Information S1) reveals that there are significant differences in representations of the TP-only SST variance among CMIP6 models.

Compared to the full SST variance, the simulations of the decadal-scale SST variance patterns in CMIP6 models are more scattered, with SCCs smaller than 0.8 and the STDs varying markedly from model to model (Figure

S13c in Supporting Information S1). This is consistent with our finding that the representation of the TPDV in CMIP6 models is significantly different from observations (Figure 1). Although most models underestimate the observed decadal-scale SST variance (Figure S13c in Supporting Information S1), most models overestimate the observed TP-only decadal SST variance (Figure S13d in Supporting Information S1). This reveals that CMIP6 models, even if able to reproduce the total SST variance pattern, exhibit significant challenges in capturing the spatial structure of TPDV along with the tropical-extratropical coupling dynamics that are key for generating TPDV. Especially, the TPDV in Group 2 models seems to be dominated by local dynamics, showing weak coupling with the extra-tropics. Previous studies show that the contribution of the tropical-extratropical feedback to the TPDV possibly depends on the decadal background state (e.g., Jia et al., 2021). The different decadal background states may be an important factor leading to the large discrepancy in the TP-only decadal SST variance among the CMIP6 models (Figure S13d in Supporting Information S1), which is worth exploring in future work.

The discrepancy between the CMIP6 patterns and observations exceeds 90% of the LIM samples (Figure S13 in Supporting Information S1, dark gray dots), suggesting that the differences between the model and observed tropical Pacific SST variance are statistically significant. The differences are likely due to the model error rather than the limitation of a single observational realization. This is even true for the MEM SST variance patterns (blue, green, and red pentagrams in Figure S13 in Supporting Information S1).

We have also explored the role of thermocline variability and surface fluxes in driving TPDV. In observations, the thermodynamical coupling processes inject energy into the central tropical Pacific, which is then transferred to the eastern tropical Pacific by the tropical dynamical processes to form the TPDV pattern. However, most CMIP6 models cannot capture the correct location where thermodynamical coupling influences TPDV, and greatly underestimate the contribution of thermocline variability (Figure 4).

Previous studies suggest that dynamics in the North and South Pacific may play different roles in the tropical Pacific climate variability (Liguori & Di Lorenzo, 2019). To follow up on this study, we could separate the roles of the northern and southern extratropical Pacific in TPDV and explore their relative contributions in both observations and climate models using the LIM diagnostic method.

While there is a long set of literature discussing the non-linearities of ENSO, the tropical-extratropical dynamics that have been uncovered in the literature to date are mostly linear in nature (e.g., atmospheric and oceanic Rossby waves, Meridional Models, TWC), which are well captured by the LIM. Having said that, there is still potential for non-linear dynamics may play some role that is yet to be identified. The LIM can capture some nonlinear dynamics, for the dynamical operator L includes linearly parameterizable nonlinear dynamics, and the stochastic forcing term encapsulates all remaining unpredictable nonlinear dynamics. Even though, the tropical Pacific climate variability may include nonlinearities that LIM cannot capture. As such, the role of the nonlinear processes needs to be further examined using nonlinear models (e.g., coupled general circulation models).

Taken together, these results suggest that despite the models' ability to simulate ENSO-scale variability in the tropical Pacific, significant challenges exist across models in reproducing the observed dynamics and patterns of TPDV. These differences are outside the range of natural internal TPDV noise and pose important questions regarding our ability to model the impacts of natural internal low-frequency variability on long-term climate change.

Data Availability Statement

The ORAS4 output can be downloaded from: <https://www.cen.uni-hamburg.de/en/icdc/data/ocean/easy-init-ocean/ecmwf-ocean-reanalysis-system-4-oras4.html>. The CMIP6 models used in this work are listed in Table S1 in Supporting Information S1. The model data were obtained from <https://esgf-node.llnl.gov/projects/cmip6/>.

References

- Alexander, M. A., Bladé, I., Newman, M., Lanzante, J. R., Lau, N.-C., & Scott, J. D. (2002). The atmospheric bridge: The influence of ENSO teleconnections on air–sea interaction over the global oceans. *Journal of Climate*, 15(16), 2205–2231. [https://doi.org/10.1175/1520-0442\(2002\)015<2205:tabtio>2.0.co;2](https://doi.org/10.1175/1520-0442(2002)015<2205:tabtio>2.0.co;2)
- An, S.-I., & Jin, F. F. (2001). Collective role of thermocline and zonal advective feedbacks in the ENSO mode. *Journal of Climate*, 14(16), 3421–3432. [https://doi.org/10.1175/1520-0442\(2001\)014<3421:crotaz>2.0.co;2](https://doi.org/10.1175/1520-0442(2001)014<3421:crotaz>2.0.co;2)
- Anderson, B. T., Perez, R. C., & Karspeck, A. (2013). Triggering of El Niño onset through trade wind-induced charging of the equatorial Pacific. *Geophysical Research Letters*, 40(6), 1212–1216. <https://doi.org/10.1002/grl.50200>

Acknowledgments

We thank two reviewers and the editor for their constructive comments on this paper. This work is supported by the National Natural Science Foundation of China (No. 42206025), the Taishan Scholars Program, and the U.S. Department of Energy's Regional and Global Model Analysis program (No. DE-SC0023228).

- Balmaseda, M. A., Mogensén, K., & Weaver, A. T. (2013). Evaluation of the ECMWF ocean reanalysis system ORAS4. *Quarterly Journal of the Royal Meteorological Society*, 139(674), 1132–1161. <https://doi.org/10.1002/qj.2063>
- Capotondi, A., Deser, C., Phillips, A. S., Okumura, Y., & Larson, S. M. (2020). ENSO and Pacific decadal variability in the community Earth system model version 2. *Journal of Advances in Modeling Earth Systems*, 12, e2019MS002022. <https://doi.org/10.1029/2019ms002022>
- Capotondi, A., & Qiu, B. (2022). Decadal variability of the Pacific shallow overturning circulation and the role of local wind forcing. *Journal of Climate*.
- Chang, P., Zhang, L., Saravanan, R., Vimont, D. J., Chiang, J. C. H., Ji, L., et al. (2007). Pacific meridional mode and El Niño-southern oscillation. *Geophysical Research Letters*, 34(16). <https://doi.org/10.1029/2007gl030302>
- Chiang, J. C. H., & Vimont, D. J. (2004). Analogous Pacific and Atlantic meridional modes of tropical atmosphere-ocean variability. *Journal of Climate*, 17(21), 4143–4158. <https://doi.org/10.1175/jcli4953.1>
- Chung, C. T. Y., Power, S. B., Sullivan, A., & Delage, F. (2019). The role of the South Pacific in modulating tropical Pacific variability. *Scientific Reports*, 9(1), 18311. <https://doi.org/10.1038/s41598-019-52805-2>
- Deser, C., Alexander, M. A., Xie, S. P., & Phillips, A. S. (2010). Sea surface temperature variability: Patterns and mechanisms. *Annual Review of Marine Science*, 2, 115–143. <https://doi.org/10.1146/annurev-marine-120408-151453>
- Di Lorenzo, E., Combes, V., Keister, J., Strub, P. T., Thomas, A., Franks, P., et al. (2013). Synthesis of Pacific Ocean climate and ecosystem dynamics. *Oceanography*, 26(4), 68–81. <https://doi.org/10.5670/oceanog.2013.76>
- Di Lorenzo, E., Liguori, G., Schneider, N., Furtado, J. C., Anderson, B. T., & Alexander, M. A. (2015). ENSO and meridional modes: A null hypothesis for Pacific climate variability. *Geophysical Research Letters*, 42(21), 9440–9448. <https://doi.org/10.1002/2015gl066281>
- Ding, R., Li, J., & Tseng, Y. (2015). The impact of South Pacific extratropical forcing on ENSO and comparisons with the North Pacific. *Climate Dynamics*, 44(7–8), 2017–2034. <https://doi.org/10.1007/s00382-014-2303-5>
- England, M. H., McGregor, S., Spence, P., Meehl, G. A., Timmermann, A., Cai, W. J., et al. (2014). Recent intensification of wind-driven circulation in the Pacific and the ongoing warming hiatus. *Nature Climate Change*, 4(3), 222–227. <https://doi.org/10.1038/nclimate2106>
- Eyring, V., Bony, S., Meehl, G. A., Senior, C. A., Stevens, B., Stouffer, R. J., & Taylor, K. E. (2016). Overview of the coupled model inter-comparison project phase 6 (CMIP6) experimental design and organization. *Geoscientific Model Development*, 9(5), 1937–1958. <https://doi.org/10.5194/gmd-9-1937-2016>
- Fisman, D. N., Tuite, A. R., & Brown, K. A. (2016). Impact of El Niño Southern Oscillation on infectious disease hospitalization risk in the United States. *Proceedings of the National Academy of Sciences of the United States of America*, 113(51), 14589–14594. <https://doi.org/10.1073/pnas.1604980113>
- Frankignoul, C., Gastineau, G., & Kwon, Y. O. (2017). Estimation of the SST response to anthropogenic and external forcing and its impact on the Atlantic multidecadal oscillation and the Pacific decadal oscillation. *Journal of Climate*, 30(24), 9871–9895. <https://doi.org/10.1175/jcli-d-17-0009.1>
- Hasselmann, K. (1976). Stochastic climate models Part I. Theory. *Tellus*, 28(6), 473–485. <https://doi.org/10.1111/j.2153-3490.1976.tb00696.x>
- Henley, B. J., Meehl, G., Power, S. B., Folland, C. K., King, A. D., Brown, J. N., et al. (2017). Spatial and temporal agreement in climate model simulations of the interdecadal Pacific Oscillation. *Environmental Research Letters*, 12(4), 044011. <https://doi.org/10.1088/1748-9326/aac5c8>
- Jia, F., Cai, W., Gan, B., Wu, L., & Di Lorenzo, E. (2021). Enhanced North Pacific impact on El Niño/Southern Oscillation under greenhouse warming. *Nature Climate Change*, 11(10), 840–847. <https://doi.org/10.1038/s41558-021-01139-x>
- Jin, F.-F., & An, S.-I. (1999). Thermocline and zonal advective feedbacks within the equatorial ocean recharge oscillator model for ENSO. *Geophysical Research Letters*, 26(19), 2989–2992. <https://doi.org/10.1029/1999gl002297>
- Kosaka, Y., & Xie, S. P. (2013). Recent global-warming hiatus tied to equatorial Pacific surface cooling. *Nature*, 501(7467), 403–407. <https://doi.org/10.1038/nature12534>
- Li, C., Wang, D., Liang, J., Gu, D., & Liu, Y. (2006). Local positive feedback of the tropical Pacific ocean-atmosphere system on interdecadal timescales. *Chinese Science Bulletin*, 51(5), 601–606. <https://doi.org/10.1007/s11434-006-0601-y>
- Liguori, G., & Di Lorenzo, E. (2019). Separating the North and South Pacific meridional modes contributions to ENSO and tropical decadal variability. *Geophysical Research Letters*, 46(2), 906–915. <https://doi.org/10.1029/2018gl080320>
- Liu, Z., & Di Lorenzo, E. (2018). Mechanisms and predictability of Pacific decadal variability. *Current Climate Change Reports*, 4(2), 128–144. <https://doi.org/10.1007/s40641-018-0090-5>
- Liu, Z., Wu, L., Gallimore, R., & Jacob, R. (2002). Search for the origins of Pacific decadal climate variability. *Geophysical Research Letters*, 29(10), 1404–1442. <https://doi.org/10.1029/2001gl013735>
- Liu, Z., & Xie, S. P. (1994). Equatorward propagation of coupled air-sea disturbances with application to the annual cycle of the eastern tropical Pacific. *Journal of the Atmospheric Sciences*, 51(24), 3807–3822. [https://doi.org/10.1175/1520-0469\(1994\)051<3807:epocad>2.0.co;2](https://doi.org/10.1175/1520-0469(1994)051<3807:epocad>2.0.co;2)
- Lou, J., O’Kane, T. J., & Holbrook, N. J. (2020). A linear inverse model of tropical and south Pacific seasonal predictability. *Journal of Climate*, 33(11), 4537–4554. <https://doi.org/10.1175/jcli-d-19-0548.1>
- Lou, J., O’Kane, T. J., & Holbrook, N. J. (2021). A linear inverse model of tropical and south Pacific climate variability: Optimal structure and stochastic forcing. *Journal of Climate*, 34(1), 143–155. <https://doi.org/10.1175/jcli-d-19-0964.1>
- Lyu, K., Zhang, X., Church, J. A., & Hu, J. (2016). Evaluation of the interdecadal variability of sea surface temperature and sea level in the Pacific in CMIP3 and CMIP5 models. *International Journal of Climatology*, 36(11), 3723–3740. <https://doi.org/10.1002/joc.4587>
- Meehl, G. A., Hu, A. X., Arblaster, J. M., Fasullo, J., & Trenberth, K. E. (2013). Externally forced and internally generated decadal climate variability associated with the interdecadal Pacific oscillation. *Journal of Climate*, 26(18), 7298–7310. <https://doi.org/10.1175/jcli-d-12-00548.1>
- Newman, M., Alexander, M. A., Ault, T. R., Cobb, K. M., Deser, C., Di Lorenzo, E., et al. (2016). The Pacific decadal oscillation, revisited. *Journal of Climate*, 29(12), 4399–4427. <https://doi.org/10.1175/jcli-d-15-0508.1>
- Okumura, Y. M. (2013). Origins of tropical Pacific decadal variability: Role of stochastic atmospheric forcing from the South Pacific. *Journal of Climate*, 26(24), 9791–9796. <https://doi.org/10.1175/jcli-d-13-00448.1>
- Penland, C., & Matrosova, L. (2016). Studies of El Niño and interdecadal variability in tropical sea surface temperatures using a nonnormal filter. *Journal of Climate*, 19(22), 5796–5815. <https://doi.org/10.1175/jcli3951.1>
- Penland, C., & Sardeshmukh, P. D. (1995). The optimal-growth of tropical sea-surface temperature anomalies. *Journal of Climate*, 8(8), 1999–2024. [https://doi.org/10.1175/1520-0442\(1995\)008<1999:togots>2.0.co;2](https://doi.org/10.1175/1520-0442(1995)008<1999:togots>2.0.co;2)
- Power, S., Casey, T., Folland, C., Colman, A., & Mehta, V. (1999). Interdecadal modulation of the impact of ENSO on Australia. *Climate Dynamics*, 15(5), 319–324. <https://doi.org/10.1007/s003820050284>
- Power, S., Lengaigne, M., Capotondi, A., Khodri, M., Vialard, J., Jebri, B., et al. (2021). Decadal climate variability in the tropical Pacific: Characteristics, causes, predictability, and prospects. *Science*, 374(6563), eaay9165. <https://doi.org/10.1126/science.aay9165>
- Sun, T., & Okumura, Y. M. (2019). Role of stochastic atmospheric forcing from the South and North Pacific in tropical Pacific decadal variability. *Journal of Climate*, 32(13), 4013–4038. <https://doi.org/10.1175/jcli-d-18-0536.1>

- Vimont, D., Wallace, J., & Battisti, D. (2003). The seasonal footprinting mechanism in the Pacific: Implications for ENSO. *Journal of Climate*, 16, 2668–2675. [https://doi.org/10.1175/1520-0442\(2003\)016<2668:tsfmit>2.0.co;2](https://doi.org/10.1175/1520-0442(2003)016<2668:tsfmit>2.0.co;2)
- Vimont, D. J. (2005). The contribution of the interannual ENSO cycle to the spatial pattern of decadal ENSO-like variability. *Journal of Climate*, 18(12), 2080–2092. <https://doi.org/10.1175/JCLI3365.1>
- Vimont, D. J., Battisti, D. S., & Hirst, A. C. (2001). Footprinting: A seasonal connection between the tropics and mid-latitudes. *Geophysical Research Letters*, 28(20), 3923–3926. <https://doi.org/10.1029/2001gl013435>
- Watanabe, M., Shiogama, H., Tatebe, H., Hayashi, M., Ishii, M., & Kimoto, M. (2014). Contribution of natural decadal variability to global warming acceleration and hiatus. *Nature Climate Change*, 4(10), 893–897. <https://doi.org/10.1038/nclimate2355>
- Wu, L., Liu, Z., Gallimore, R., Jacob, R., Lee, D., & Zhong, Y. (2003). Pacific decadal variability: The tropical Pacific mode and the North Pacific mode. *Journal of Climate*, 16(8), 1101–1120. [https://doi.org/10.1175/1520-0442\(2003\)16<1101:pdvttp>2.0.co;2](https://doi.org/10.1175/1520-0442(2003)16<1101:pdvttp>2.0.co;2)
- Xie, S.-P., & Philander, S. (1994). A coupled ocean-atmosphere model of relevance to the ITCZ in the eastern Pacific. *Tellus*, 46A, 340–350
- Zhang, H., Clement, A., & Di Nezio, P. (2014). The South Pacific meridional mode: A mechanism for ENSO-like variability. *Journal of Climate*, 27(2), 769–783. <https://doi.org/10.1175/jcli-d-13-00082.1>
- Zhang, Y., Wallace, J. M., & Battisti, D. S. (1997). ENSO-like interdecadal variability: 1900–93. *Journal of Climate*, 10(5), 1004–1020. [https://doi.org/10.1175/1520-0442\(1997\)010<1004:eliv>2.0.co;2](https://doi.org/10.1175/1520-0442(1997)010<1004:eliv>2.0.co;2)
- Zhao, Y., Di Lorenzo, E., Sun, D., & Stevenson, S. (2021). Tropical Pacific decadal variability and ENSO precursor in CMIP5 models. *Journal of Climate*, 34(3), 1023–1045. <https://doi.org/10.1175/jcli-d-20-0158.1>
- Zhao, Y., & Di Lorenzo, E. (2020). The impacts of extra-tropical ENSO Precursors on tropical Pacific decadal-scale variability. *Scientific Reports*, 10(1), 12. <https://doi.org/10.1038/s41598-020-59253-3>
- Zhao, Y., Newman, M., Capotondi, A., Di Lorenzo, E., & Sun, D. (2021). Removing the effects of tropical dynamics from north pacific climate variability. *Journal of Climate*, 34(23), 9249–9265. <https://doi.org/10.1175/jcli-d-21-0344.1>